AIAA JOURNAL
Vol. 41, No. 6, June 2003

Nonequilibrium Turbulent-Viscosity Model for Supersonic Free-Shear Layer/Wall-Bounded Flows

Akira Yoshizawa*
University of Tokyo, Tokyo 153-8505, Japan
Hitoshi Fujiwara†
National Aerospace Laboratory, Tokyo 182-0012, Japan
Fujihiro Hamba‡ and Shoiti Nisizima§
University of Tokyo, Tokyo 153-8505, Japan
and
Yukihiro Kumagai¶
Japan Meteorological Agency, Tokyo 100-8122, Japan

A Reynolds mean turbulence model is presented, with attention focused on the applicability to supersonic free-shear layer and wall-bounded flows. In this model, the Reynolds stress is approximated by a nonequilibrium turbulent-viscosity representation dependent on the Lagrange derivative of turbulence quantities. Supersonic effects occur, besides the mean-density variation, in the combination of nonequilibrium and turbulent Mach number effects. Through the test in free-shear and boundary-layer flows, the proposed model is confirmed to reproduce the reduction in the growth rate of a free-shear layer flow, without causing undesirable supersonic effects on wall-bounded flows such as channel and boundary-layer flows in which the nonequilibrium effects vanish or become weak.

Nomenclature

$\bar{a}$	=	local mean sound velocity
$\mathrm{D}/\mathrm{D}t$	=	Lagrange derivation based on the mean velocity
e	=	internal energy
$\hat{f}$, f'	=	mass-weighted mean of f and fluctuation
G_N	=	normalized growth rate of a free-shear layer
$\boldsymbol{H}$	=	turbulent internal-energy flux
K	=	turbulent energy
M_C	=	convective Mach number
M_G	=	gradient Mach number
M_T	=	turbulent Mach number
P_K	=	production rate of turbulent energy
p	=	pressure
R_{ij}	=	Reynolds stress
s_{ij}	=	velocity strain tensor
$\boldsymbol{T}_K$	=	transport rate of turbulent energy
$\boldsymbol{u}$	=	velocity
δ	=	width of a free-shear layer or a boundary layer
ε	=	energy dissipation rate
θ	=	temperature
ν_T	=	turbulent viscosity
ν_{TE}	=	equilibrium turbulent viscosity
ρ	=	density
χ	=	nondimensional nonequilibrium parameter

I. Introduction

TURBULENCE modeling of supersonic flows is a challenging subject, both from practical and academic viewpoints. A typical supersonic effect is the drastic reduction in the growth rate of a plane free-shear layer flow. The reduction has been confirmed in a number of experiments under various conditions,[1] and its behavior is often characterized by the so-called Langley curve (see Ref. 2). To capture the reduction mechanism from the viewpoint of turbulence modeling, attention was first paid to the dilatational dissipation rate and the pressure–dilation correlation in the turbulent-energy equation.[3−7] In these studies, the explicit supersonic effects are represented by the turbulent Mach number. The latter effects on flow statistics were examined by the perturbation method based on weak compressibility.[8] Supersonic effects on the turbulent-energy equation were also sought in relations with the density variance.[9] All of the foregoing models succeeded in reproducing the reduction in the growth rate of a plane free-shear layer flow.

The mechanism of turbulence suppression due to supersonic effects has been clarified by the direct numerical simulation (DNS) of homogeneous-shear and free-shear layer flows.[10−12] There, the dilatational energy dissipation rate and the pressure–dilatation correlation play a minor role in the turbulent energy equation, and the close relationship exists between supersonic effects and the suppression of pressure fluctuation. Such suppression leads to the decrease in the pressure–strain correlation, resulting in the reduction in the energy supply to the turbulent normal velocity component. As a result, the Reynolds stress shear component is reduced, which gives rise to the decrease in energy production. This process is a cause of the growth-rate suppression in a free-shear layer flow.

The foregoing DNS finding indicates that the second-order modeling explicitly dealing with the pressure–strain correlation is appropriate in analyzing supersonic flows by turbulence modeling. In this vein, second-order compressible models were proposed by Adumitroaie et al.[13] and Fujiwara et al.,[14] with special attention paid to the application to a free-shear layer flow. The computational burden of the second-order model, however, is heavy in analyzing complex engineering turbulent flows. To alleviate the burden, the model by Adumitroaie et al.[13] was reduced to an explicit algebraic Reynolds stress model. Such algebraic modeling may be regarded

Received 17 September 2002; revision received 22 January 2003; accepted for publication 29 January 2003.

*Professor, Institute of Industrial Science, Meguro-ku.
†Senior Research Engineer, Advanced Aircraft Research Center, Chofu.
‡Associate Professor, Institute of Industrial Science, Meguro-ku.
§Research Associate, Institute of Industrial Science, Meguro-ku.
¶Technical Officer, Numerical Prediction Division, Chiyoda-ku.

as a mathematical compromise between the proper treatment of anisotropy of turbulent intensities and the manageability of models.

Supersonic effects occur quite differently in wall-bounded flows such as channel and boundary-layer flows. In the DNS[15] of a supersonic isothermal-wall channel flow, the density variance is large, specifically near the wall, but the pressure variance is very small over the whole region. The mean velocity can be expressed by the logarithmic velocity law with the mean-density variation taken into account through the van Driest transformation. This indicates that, for identifying supersonic effects, pressure fluctuation is more appropriate than density fluctuation[16] and that it is important to distinguish between acoustic and entropy modes of compressible flow.[17,18] An entirely similar situation holds for a supersonic turbulent boundary-layer flow.

The foregoing discussions on free-shear layer and wall-bounded flows imply that any new compressible turbulence model needs to fulfill the following:

1) In wall-bounded flows such as channel and boundary-layer flows, supersonic effects on the mean flow appear through the change of mean density; namely, newly added turbulent supersonic effects vanish or become weak in the calculation of such flows.

2) The model may reproduce the reduction in the growth rate of a free-shear layer flow.

The current models do not always fulfill these two requirements simultaneously. For instance, the models with the dilatational dissipation rate incorporated into the turbulent-energy equation can properly reproduce the growth rate reduction in a free-shear layer flow, but they cause undesirable supersonic effects in a channel flow.

In this work, we attempt to construct a turbulence model for analyzing supersonic flows within the framework of a turbulent-viscosity representation for the Reynolds stress. Such an attempt does not seem consistent with the DNS finding that supersonic effects on turbulent flow are closely related to the pressure fluctuation and that they enhance the anisotropy of the Reynolds stress through the pressure–strain correlation. With this point in mind, we study a turbulent-viscosity model from the following standpoint:

1) In explicit algebraic Reynolds stress modeling, the turbulent-viscosity part is still the leading term, and turbulent supersonic effects inevitably occur there, as is seen from the model by Adumitroaie et al.[13] Then a turbulent-viscosity model capturing some properties of both of supersonic free-shear layer and wall-bounded flows is expected to give a useful clue as to the further development of explicit algebraic modeling of supersonic flows.

2) In analyzing flows encountered in aeronautical and mechanical engineering, the simplicity of a turbulence model is one of the important requisites for reducing the computational burden arising from high Reynolds number and complicated flow geometry. The concept of turbulent viscosity and diffusivity leads to mathematically simple modeling of turbulence.

This paper is organized as follows. The fundamental equations for a compressible flow are given in Sec. II. The nonequilibrium effect on the turbulent viscosity is explained in Sec. III. In Sec. IV, the combination of nonequilibrium and turbulent Mach number effects is proposed for modeling supersonic effects, and its physical meaning is discussed in light of the DNS findings. In Sec. V, the proposed model is applied to free-shear and boundary-layer flows. The conclusions are given in Sec. VI.

II. Compressible-Flow Equations

A. Fundamental Equations

The three equations governing the motion of a viscous, compressible fluid consist of the following:

$$\frac{\partial \rho}{\partial t} + \nabla \cdot (\rho \boldsymbol{u}) = 0 \tag{1}$$

$$\frac{\partial}{\partial t}\rho u_i + \frac{\partial}{\partial x_j}\rho u_i u_j = -\frac{\partial p}{\partial x_i} + \frac{\partial}{\partial x_j}\mu s_{ij} \tag{2}$$

$$\frac{\partial}{\partial t}\rho e + \nabla \cdot (\rho \boldsymbol{u} e) = -p\nabla \cdot \boldsymbol{u} + \nabla \cdot (\kappa \nabla \theta) + \phi \tag{3}$$

Here, μ is the viscosity and κ is the thermal conductivity. The traceless part of the velocity strain tensor s_{ij} is defined as

$$s_{ij} = \frac{\partial u_j}{\partial x_i} + \frac{\partial u_i}{\partial x_j} - \frac{2}{3}\nabla \cdot \boldsymbol{u}\delta_{ij} \tag{4}$$

and the dissipation function ϕ will be neglected in what follows. Under the perfect-gas assumption, we have the relation

$$p = (\gamma - 1)\rho e \tag{5}$$

with

$$e = C_V \theta \tag{6}$$

where C_V is the specific heat at constant volume and γ is the ratio of the specific heat at constant temperature C_P, to C_V.

B. Mass-Weighted Ensemble-Mean System

In modeling low-Mach-number turbulent flows, we usually apply the simple ensemble averaging to a system of fundamental equations. In the compressible case, however, the advection-related parts in Eqs. (1–3), which are of the third order in ρ, $\boldsymbol{u}$, and e, bring several extra correlation terms linked with density fluctuation. A method for avoiding this complexity is the use of the mass-weighted ensemble averaging. There the mean of a quantity f and the fluctuation around it are defined by

$$\hat{f} = \{f\}_M \equiv \langle \rho f \rangle / \bar{\rho}, \qquad \bar{\rho} = \langle \rho \rangle \tag{7}$$

$$f' = f - \hat{f} \tag{8}$$

respectively, where subscript $\boldsymbol{M}$ signifies mass-weighted, $\langle\,\rangle$ denotes the ensemble mean, and

$$f = (\boldsymbol{u}, p, e) \tag{9}$$

We apply Eq. (7) to Eqs. (1–3) and have

$$\frac{\partial \bar{\rho}}{\partial t} + \nabla \cdot (\bar{\rho}\hat{\boldsymbol{u}}) = 0 \tag{10}$$

$$\frac{\partial}{\partial t}\bar{\rho}\hat{u}_i + \frac{\partial}{\partial x_j}\bar{\rho}\hat{u}_i\hat{u}_j = -\frac{\partial \bar{p}}{\partial x_i} + \frac{\partial}{\partial x_j}(-\bar{\rho}R_{ij}) \tag{11}$$

$$\frac{\partial}{\partial t}\bar{\rho}\hat{e} + \nabla \cdot (\bar{\rho}\hat{\boldsymbol{u}}\hat{e}) = -\langle p\nabla \cdot \boldsymbol{u}\rangle + \nabla \cdot (-\bar{\rho}\boldsymbol{H}) \tag{12}$$

where the mass-weighted Reynolds stress and internal-energy flux, R_{ij} and $\boldsymbol{H}$, are

$$R_{ij} = \{u'_i u'_j\}_M \tag{13}$$

$$\boldsymbol{H} = \{e'\boldsymbol{u}'\}_M \tag{14}$$

and the molecular-diffusion terms related to μ and κ were dropped because they do not play an important role, except as discussed in Sec. V.B. The ensemble-mean pressure $\bar{p}$ in Eq. (11) may be rewritten as

$$\bar{p} = \langle(\gamma - 1)\rho e\rangle = (\gamma - 1)\bar{\rho}\hat{e} \tag{15}$$

For $\langle p\nabla \cdot \boldsymbol{u}\rangle$, we make the simplest approximation

$$\langle p\nabla \cdot \boldsymbol{u}\rangle \cong \bar{p}\nabla \cdot \hat{\boldsymbol{u}} = (\gamma - 1)\bar{\rho}\hat{e}\nabla \cdot \hat{\boldsymbol{u}} \tag{16}$$

III. Modeling of Turbulent Viscosity at Low Mach Numbers

A. Nonequilibrium Effects

In this work, we express the Reynolds stress R_{ij} and the turbulent internal-energy flux $\boldsymbol{H}$ with the aid of transport coefficients and aim at constructing as simple a model as possible. In the low-Mach-number limit, we do not need to distinguish the mass-weighted ensemble averaging from the simple ensemble averaging; namely, we may take $\langle f \rangle = \{f\}_M \equiv \hat{f}$. With this in mind, we write

$$R_{ij} = \tfrac{2}{3} K \delta_{ij} - \nu_T \hat{s}_{ij} \tag{17}$$

$$\boldsymbol{H} = -(\nu_T/\sigma_e)\nabla\hat{e} \tag{18}$$

where $\hat{s}_{ij} = \{s_{ij}\}_M$ with $\nabla\cdot\hat{\boldsymbol{u}}$ dropped. In the standard $K-\varepsilon$ model, the turbulent viscosity ν_T is written most simply as

$$\nu_T = \nu_{\mathrm{TE}} \equiv C_\nu (K^2/\varepsilon) \tag{19}$$

where K and ε are defined as

$$K = \left\{\frac{1}{2}\boldsymbol{u}'^2\right\}_M \left(\left\langle \frac{1}{2}\boldsymbol{u}'^2 \right\rangle\right) \tag{20}$$

$$\varepsilon = \bar{\nu}\left\{\left(\frac{\partial u'_j}{\partial x_i} + \frac{\partial u'_i}{\partial x_j} - \frac{2}{3}\nabla\cdot\boldsymbol{u}'\delta_{ij}\right)\frac{\partial u'_j}{\partial x_i}\right\}_M, \qquad \left[\bar{\nu}\left\langle\left(\frac{\partial u'_j}{\partial x_i}\right)^2\right\rangle\right] \tag{21}$$

with $\bar{\nu} = \bar{\mu}/\bar{\rho}$. (The expressions in the last parentheses correspond to those at low Mach numbers.) The nondimensional factor C_ν is usually chosen as

$$C_\nu = 0.09 \tag{22}$$

In Eq. (19), subscript E denotes equilibrium, whose meaning will be explained later. In Eq. (18), σ_e is a positive nondimensional coefficient and is usually chosen to be a constant.

Let us consider Eq. (19) in light of the Kolmogorov scaling, familiar in the study of isotropic turbulence. From a dimensional consideration, we write

$$\nu_{\mathrm{TE}} = |\boldsymbol{u}'|\ell = \sqrt{\boldsymbol{K}}\ell \tag{23}$$

apart from numerical factors, where $|\boldsymbol{u}'|$ is the intensity of velocity fluctuation and ℓ is the characteristic length of energy-containing eddies such as the integral length. We estimate the turbulent energy K with the aid of the Kolmogorov $-\frac{5}{3}$ power spectrum, and have

$$K = \int_{k \geq O(\ell^{-1})} \varepsilon^{\frac{2}{3}} k^{-\frac{5}{3}}\,\mathrm{d}k = (\ell\varepsilon)^{\frac{2}{3}} \tag{24a}$$

or

$$\ell = \ell_K \equiv K^{\frac{3}{2}}/\varepsilon \tag{24b}$$

except numerical factors, where ℓ_K is named the Kolmogorov-scaling length. Equations (23) and (24) result in Eq. (19).

In the low-Mach-number limit, K obeys

$$\frac{\mathrm{D}K}{\mathrm{D}t} \equiv \left(\frac{\partial}{\partial t} + \hat{\boldsymbol{u}}\cdot\nabla\right)K = P_K - \varepsilon + \nabla\cdot\boldsymbol{T}_K \tag{25}$$

Here P_K and $\boldsymbol{T}_K$ are the energy production and transport rates, respectively, which are defined by

$$P_K = -R_{ij}\frac{\partial \hat{u}_j}{\partial x_i} \tag{26}$$

$$\boldsymbol{T}_K = -\left\langle\left(\frac{1}{2}\boldsymbol{u}'^2 + \frac{1}{\bar{\rho}}p'\right)\boldsymbol{u}'\right\rangle \tag{27}$$

The Kolmogorov scaling is based on the equilibrium property of turbulence, that is, the quasi balance between the energy supply and dissipation rates. This state may be regarded as $P_K \cong \varepsilon$ in the context of Eq. (25).

Typical flows whose prominent feature is $P_K > \varepsilon$ are temporally and spatially developing homogeneous-shear turbulences. These two flows are similar to each other in the sense that the turbulence statistics of one flow may be estimated from the counterparts of the other through the coordinate transformation $t = x/U$. (U is the mean velocity in the x direction.) In the use of the standard $K-\varepsilon$ model based on Eq. (19), the growth of K and ε in a temporally developing homogeneous-shear flow is overestimated, compared with the DNS counterparts. (The quantitative discussion is given in Refs. 19 and 20.) A free-shear layer flow, our primary concern, and a spatially developing homogeneous-shear flow share the feature that flow statistics are developing in the downstream (x) direction. This indicates that Eq. (19) needs to be treated carefully in the study of a free-shear layer flow whose properties vary in the downstream direction.

B. Nonequilibrium Turbulent-Viscosity Model

Nonequilibrium effects on the turbulent viscosity have already been examined on the basis of the results by the two-scale direct-interaction approximation (TSDIA).[21–23] From the refined version of the TSDIA,[23,24] ν_T is given by

$$\nu_T = 0.12\frac{K^2}{\varepsilon}\left[1 - 0.76\left(1.6\frac{1}{\varepsilon}\frac{\mathrm{D}K}{\mathrm{D}t} - \frac{K}{\varepsilon^2}\frac{\mathrm{D}\varepsilon}{\mathrm{D}t}\right)\right] \tag{28a}$$

$$\nu_T \cong 0.12\frac{K^2}{\varepsilon}\left(1 - 0.8\frac{1}{K}\frac{\mathrm{D}}{\mathrm{D}t}\frac{K^2}{\varepsilon}\right) \tag{28b}$$

In the TSDIA formalism, the D/Dt-related terms in Eq. (28) were obtained as the correction to the equilibrium turbulent viscosity ν_{TE} [Eq. (19)]. In a numerical sense, the numerical coefficient 0.12 is estimated to be about 30% larger than that of Eq. (22) or the value optimized through the application to a channel flow.

In flows subject to a strong mean velocity shear, the overestimate of K is a typical defect of the equilibrium viscosity ν_{TE} [Eq. (19)]. There, we often have

$$\frac{1}{K}\frac{\mathrm{D}}{\mathrm{D}t}\frac{K^2}{\varepsilon} > 0 \tag{29}$$

as is the case in homogeneous-shear turbulence. The D/Dt effect in Eq. (28) is instrumental in rectifying the overestimate of the turbulent-energy production that arises from ν_{TE}. In the computation of general turbulent flows, large positive $(1/K)\mathrm{D}(K^2/\varepsilon)/\mathrm{D}t$ may occur locally and give rise to an unphysical negative viscosity. To avoid this difficulty and enlarge the applicability of Eq. (28b), we use the simplest Padé approximation for positive $\mathrm{D}(K^2/\varepsilon)/\mathrm{D}t$ and adopt

$$\nu_T = \nu_{\mathrm{TE}}\Bigg/\left(1 + C_N\frac{1}{K}\frac{\mathrm{D}}{\mathrm{D}t}\frac{K^2}{\varepsilon}\right) \qquad \text{for} \qquad \frac{\mathrm{D}}{\mathrm{D}t}\frac{K^2}{\varepsilon} > 0 \tag{30a}$$

$$\nu_T = \left(1 - C_N\frac{1}{K}\frac{\mathrm{D}}{\mathrm{D}t}\frac{K^2}{\varepsilon}\right)\nu_{\mathrm{TE}}, \qquad \text{for} \qquad \frac{\mathrm{D}}{\mathrm{D}t}\frac{K^2}{\varepsilon} < 0 \tag{30b}$$

Negative $\mathrm{D}(K^2/\varepsilon)/\mathrm{D}t$ may occur in cases such as a converging–diverging nozzle, and Eq. (30a) is likely to produce singularity. In such a situation, the original form and Eq. (30b) are candidates of ν_T and need to be tested.

In the analysis of homogeneous-shear turbulence,[19] Eq. (30a) has already been proven to rectify the shortfall of Eq. (19). In the work in Ref. 19, the choice of $C_N = 1.3$ was shown to reproduce K and ε consistent with the DNS based on the initial nondimensional shear rate $KS_\infty/\varepsilon \cong 28$. This shear rate, however, is much larger than the rates usually encountered in nearly homogeneous-shear turbulent flows. For the latter, we have $KS_\infty/\varepsilon < 10$, and a smaller C_N suffices for reproducing K and ε properly. In the present work, we adopt the theoretically suggested value $C_N = 0.8$.

We substitute the standard $K-\varepsilon$ model for an incompressible flow into the denominator of Eq. (30a) and neglect the diffusion effects. Then we have the prototype of a nonequilibrium turbulent-viscosity model. More elaborate explicit algebraic nonlinear models have been proposed for incorporating the properties intrinsic to the Reynolds stress equation.[25–29] A prominent feature of Eq. (30) is that the nonequilibrium effect expressed by $\mathrm{D}/\mathrm{D}t$ vanishes identically in the channel flow. The importance of this property for fulfilling the requirement 1 in Sec. I will be shown.

IV. Modeling of Supersonic Effects

A. Relationship Between Streamwise Variation and Supersonic Effects

A representative nondimensional parameter of a supersonic turbulent flow is the turbulent Mach number

$$M_T = \sqrt{\langle u'^2\rangle}\Big/\bar{a} = \sqrt{2K}\Big/\bar{a} \tag{31}$$

Here, $\bar{a}$ is given by

$$\bar{a} = \sqrt{\frac{\mathrm{d}\bar{p}}{\mathrm{d}\bar{\rho}}} = \sqrt{\gamma(\gamma-1)\hat{e}} \tag{32}$$

from Eq. (15) and the adiabatic condition. When the dilatational dissipation, the pressure–dilatation correlation, and the pressure–strain correlation were modeled, M_T was adopted as one of the primary nondimensional parameters characterizing supersonic effects, as was noted in Sec. I.[3–9,13,14]

The turbulent Mach number M_T increases with a mainstream Mach number. Large M_T itself, however, is not always linked with turbulent supersonic effects. It typically relates to a supersonic channel flow.[15] There, the density fluctuation is high near the wall, but the logarithmic velocity profile may be explained though the inclusion of mean-density variation. A factor distinguishing a channel flow from a free-shear layer flow is the streamwise change of flow quantities. In a supersonic flow, the streamwise change of flow is a primary generator of fluid compression, that is, the occurrence of pressure variation.

Representative quantities characterizing the degree of streamwise change are Lagrange derivatives such as $\mathrm{D}K/\mathrm{D}t$. In reality, $\mathrm{D}K/\mathrm{D}t$ vanishes identically in a channel flow, whereas nonvanishing $\mathrm{D}K/\mathrm{D}t$ is one of the features of a free-shear layer flow. In a turbulent boundary-layer flow, $\mathrm{D}K/\mathrm{D}t$ survives, but its magnitude decreases with the growth of the layer. This point will be referred to later, in the application of the proposed model to a supersonic boundary-layer flow.

B. Supersonic Effects on Turbulent Viscosity

With the foregoing discussions in mind, we seek a nondimensional parameter that is capable of expressing supersonic effects on the turbulent viscosity ν_T. In the low-Mach-number limit, the streamwise-variation effect on ν_T is given by the $\mathrm{D}/\mathrm{D}t$-related part in Eq. (30). We first combine it with M_T and introduce the nondimensional parameter

$$\chi = M_T^2 \frac{1}{K}\frac{\mathrm{D}}{\mathrm{D}t}\frac{K^2}{\varepsilon} \tag{33}$$

To see the physical meaning of Eq. (33), we consider homogeneous-shear turbulence and use the standard $K-\varepsilon$ model. [The equation for ε is given by Eq. (49).] Then Eq. (33) is reduced to

$$\chi = C_\nu(2-C_{\varepsilon1})M_T^2\left[\left(\frac{KS_\infty}{\varepsilon}\right)^2 - \frac{2-C_{\varepsilon2}}{C_\nu(2-C_{\varepsilon1})}\right] \cong C_\nu(2-C_{\varepsilon1})\left(\frac{M_T K S_\infty}{\varepsilon}\right)^2 \tag{34}$$

where the second part in the parenthesis of the first relation is negligible because $KS_\infty/\varepsilon = 5.0$ in the stationary state.[30]

In the study of supersonic effects on turbulence, Sarkar[10] showed that the gradient Mach number M_G is an important parameter controlling those effects. In homogeneous-shear turbulence, it is written as

$$M_G = S_\infty \ell_C/\bar{a} \tag{35}$$

where ℓ_C is a characteristic turbulence scale. As the simplest choice of ℓ_C, we use the Kolmogorov-scaling length defined by Eq. (24b), that is,

$$\ell_C = \ell_K \tag{36}$$

The question raised by this choice will be addressed later. From Eqs. (35) and (36), we have

$$M_G = \left(\sqrt{2}/2\right)(M_T K S_\infty/\varepsilon) \tag{37}$$

We compare the second relation of Eq. (34) with Eq. (37) and find that the nondimensional parameter χ is related to M_G as

$$\chi = 2C_\nu(2-C_{\varepsilon1})M_G^2 \tag{38}$$

under the assumption of Eq. (36) and the use of the standard $K-\varepsilon$ model. Note here that the occurrence of M_T^2 in Eq. (33), but not of M_T, is reasonable under Eq. (36).

The foregoing discussion shows that χ defined by Eq. (33) is one of the nondimensional parameters characterizing supersonic effects. We are in a position to incorporate the χ effect into the nonequilibrium turbulent viscosity given by Eq. (30). Fluid compression is often linked with the streamwise change of flow properties. Then, we consider that M_T effects alter the coefficient C_N attached to the $\mathrm{D}/\mathrm{D}t$-related part, replacing C_N with $C_{NC}(M_T)$ that is a function of M_T. Specifically, we adopt a simple expression

$$C_{NC}(M_T) = C_N + C_M M_T^2 \tag{39}$$

where C_M is a model constant. Then we have

$$\nu_T = \nu_{\mathrm{TE}}\Bigg/\left[1+\left(C_N + C_M M_T^2\right)\frac{1}{K}\frac{\mathrm{D}}{\mathrm{D}t}\frac{K^2}{\varepsilon}\right] \quad \text{for} \quad \frac{\mathrm{D}}{\mathrm{D}t}\frac{K^2}{\varepsilon} > 0 \tag{40a}$$

$$\nu_T = \left[1-\left(C_N + C_M M_T^2\right)\frac{1}{K}\frac{\mathrm{D}}{\mathrm{D}t}\frac{K^2}{\varepsilon}\right]\nu_{\mathrm{TE}} \quad \text{for} \quad \frac{\mathrm{D}}{\mathrm{D}t}\frac{K^2}{\varepsilon} < 0 \tag{40b}$$

Note here that the C_M-related part is reduced to the occurrence of χ defined by Eq. (33). The M_T^4 term is not excluded there, but the M_T-related part is not expressed using only χ.

In Eq. (40), the turbulent supersonic effects related to M_T vanish identically in a channel flow, owing to $\mathrm{D}/\mathrm{D}t$. Therefore, the present model partially fulfills requirement 1 in Sec. I. The model with the $\mathrm{D}/\mathrm{D}t$-related terms replaced with the combination of M_T and the density-variance effect was proposed previously.[31] There, requirement 1 is not guaranteed a priori.

C. Relationship with Length Scale Related to Supersonic Effects

In the foregoing discussions, we adopted the Kolmogorov-scaling length ℓ_K, Eq. (24b), as ℓ_C in Eq. (35). In the DNS of an annular mixing-layer flow by Freund et al.,[12] supersonic effects are prominent at the transverse correlation length, that is, the characteristic length normal to the main stream. It decreases with the increase in the convective Mach number. It is difficult to include this anisotropic property in one-point closure modeling, specifically, in the turbulent-viscosity approximation.

To see partially the foregoing situation from one-point modeling, we take the average of the characteristic lengths in three directions and write[13]

$$\bar{\ell}_K = \alpha\left(K^{\frac{3}{2}}/\varepsilon\right) \tag{41}$$

Here, α is no longer a numerical coefficient, unlike Eq. (24b), and is instead a function of quantities related to supersonic effects such as the convective Mach number. With $\ell_C = \bar{\ell}_K$ adopted in Eq. (35), Eq. (37) is replaced with

$$M_G = \left(\sqrt{2}/2\right)\alpha(M_T K S_\infty/\varepsilon) \tag{42}$$

We are in a position to consider the relationship of the nonequilibrium turbulent-viscosity model, Eq. (40a), with Eq. (41). In light of Eq. (23), we adopt $\bar{\ell}_K$ as a characteristic length in a supersonic flow and write

$$\nu_T = C_\nu \sqrt{K}\bar{\ell}_K = \alpha \nu_{\mathrm{TE}} \tag{43}$$

where C_ν was inserted as the numerical proportional coefficient. From the comparison between Eqs. (40) and (43), we have

$$\alpha = \left[1 + \left(C_N + C_M M_T^2\right)\frac{1}{K}\frac{\mathrm{D}}{\mathrm{D}t}\frac{K^2}{\varepsilon}\right]^{-1} \quad \text{for} \quad \frac{\mathrm{D}}{\mathrm{D}t}\frac{K^2}{\varepsilon} > 0 \tag{44a}$$

$$\alpha = \left[1 - \left(C_N + C_M M_T^2\right)\frac{1}{K}\frac{\mathrm{D}}{\mathrm{D}t}\frac{K^2}{\varepsilon}\right] \quad \text{for} \quad \frac{\mathrm{D}}{\mathrm{D}t}\frac{K^2}{\varepsilon} < 0 \tag{44b}$$

as is the case for α in Eq. (41). Then, the use of the nonequilibrium model, Eq. (40), is instrumental in including supersonic effects on a characteristic turbulence length, although it is quite limited compared with the second-order modeling based on the full use of the Reynolds stress equation. For the compressible second-order modeling, readers may consult Refs. 13 and 14 and the works cited therein.

D. Summary of Nonequilibrium Model

We summarize the nonequilibrium turbulence model proposed in this work. The system of mean-field equations is given by

$$\frac{\partial \bar{\rho}}{\partial t} + \nabla \cdot (\bar{\rho}\hat{\boldsymbol{u}}) = 0 \tag{45}$$

$$\frac{\partial}{\partial t}\bar{\rho}\hat{u}_i + \frac{\partial}{\partial x_j}\bar{\rho}\hat{u}_i\hat{u}_j = -\frac{\partial \bar{p}}{\partial x_i} + \frac{\partial}{\partial x_j}(-\bar{\rho}R_{ij}) \tag{46}$$

$$\frac{\partial}{\partial t}\bar{\rho}\hat{e} + \nabla \cdot (\bar{\rho}\hat{\boldsymbol{u}}\hat{e}) = -\bar{p}\nabla \cdot \hat{\boldsymbol{u}} + \nabla \cdot (-\bar{\rho}\boldsymbol{H}) \tag{47}$$

The ensemble-mean pressure $\bar{p}$ is given by Eq. (15), and the Reynolds stress R_{ij} and the turbulent internal-energy flux $\boldsymbol{H}$ are modeled as Eqs. (17) and (18), respectively. [The turbulent viscosity ν_T is given by Eq. (40).]

The transport equations for K and ε are given by

$$\bar{\rho}\frac{\mathrm{D}K}{\mathrm{D}t} = -\bar{\rho}R_{ij}\frac{\partial \hat{u}_j}{\partial x_i} - \bar{\rho}\varepsilon + \nabla \cdot \left(\bar{\rho}\frac{\nu_{\mathrm{TE}}}{\sigma_K}\nabla K\right) \tag{48}$$

$$\bar{\rho}\frac{\mathrm{D}\varepsilon}{\mathrm{D}t} = -C_{\varepsilon 1}\frac{\varepsilon}{K}\bar{\rho}R_{ij}\frac{\partial \hat{u}_j}{\partial x_i} - C_{\varepsilon 2}\bar{\rho}\frac{\varepsilon^2}{K} + \nabla \cdot \left(\bar{\rho}\frac{\nu_{\mathrm{TE}}}{\sigma_\varepsilon}\nabla \varepsilon\right) \tag{49}$$

These two equations are of the same form as the standard incompressible $K - \varepsilon$ model, except for the appearance of $\bar{\rho}$. Namely, they are reduced to the standard $K - \varepsilon$ model under $C_N = C_M = 0$. In this model, the explicit supersonic effects only occur through ν_T in R_{ij} and $\boldsymbol{H}$.

The present model contains eight model constants:

$$C_\nu = 0.09, \qquad \sigma_K = 1, \qquad C_{\varepsilon 1} = 1.4,$$
$$C_{\varepsilon 2} = 1.9, \qquad \sigma_\varepsilon = 1.3, \qquad \sigma_e = 1 \tag{50a}$$

$$C_N = 0.8, \qquad C_M \tag{50b}$$

Of these model constants, Eq. (50a) corresponds to the set of model constants widely adopted in the K–ε model. In Eq. (50b), the first is the theoretically estimated value, and the latter will be determined through the application to a free-shear layer flow.

Here, we make three supplementary remarks. The first regards the anisotropy of the Reynolds stress. Pressure is supposed to even out anisotropy, in general. In Sec. I, the role of pressure fluctuation in generating anisotropy was referred to in light of the pressure–strain correlation. In the context of the mean pressure, the anisotropic effect proportional to $(\mathrm{D}\hat{u}_i/\mathrm{D}t)(\mathrm{D}\hat{u}_j/\mathrm{D}t)$ has recently been shown to appear in the Reynolds stress of compressible turbulence, with the aid of the statistical theory[32] based on the mass-weighted averaging. Such an effect is related to the mean pressure through Eq. (46) and may occur in a free-shear layer flow, although it disappears in a channel flow.

The second remark regards the effects of flow separation. In the presence of a large-curvature wall, vortical-flow effects arising from separation need to be incorporated into the Reynolds stress through its deviation from the isotropic-viscosity model. The DNS[33] of a turbulent flow over a rectangular trailing edge indicated that such effects become quite important in the pressure–diffusion term of the K equation. There, the term, as well as the production and advection ones, are dominant over the turbulent diffusion term. The mean-flow effects on the pressure-diffusion term were investigated on the basis of the TSDIA,[34] and its inclusion was confirmed as useful through the application to a turbulent flow over a rectangular trailing edge.[35]

The third remark regards the effects of compressibility on the ε equation. Parts of the effects may be dealt with through the first term of Eq. (49). In the present work, however, compressibility effects on the second or ε destruction term are not taken into account. It is well recognized that the destruction term needs to be modified in a rotating turbulent flow. The main part of ε is related to the square of vorticity fluctuation. This indicates that the vortex dynamics of compressible flow is expected to provide useful information about the compressibility effect on the destruction term.

V. Test of Nonequilibrium Model

A. Free-Shear Layer Flow

Let us examine the validity of the present model. For this purpose, we apply the model to a plane free-shear layer flow. We adopt the Cartesian coordinates (x, y, z), where x is along the two freestreams and y is normal to them. The flow quantities of the faster stream are denoted by attaching subscript 1, such as $(\hat{u}_1, \bar{\rho}_1, \hat{e}_1)$, whereas their slower counterparts are denoted by subscript 2.

The two freestreams are characterized by the ratios

$$\gamma_u = \hat{u}_2/\hat{u}_1, \qquad \gamma_\rho = \bar{\rho}_2/\bar{\rho}_1, \qquad \gamma_e = \hat{e}_2/\hat{e}_1 \tag{51}$$

The most important parameter characterizing Mach number effects on a free-shear layer flow is the convective Mach number, which is defined by

$$M_C = \frac{\hat{u}_1 - \hat{u}_2}{\bar{a}_1 + \bar{a}_2} \tag{52}$$

We introduce the normalized velocity in the x direction:

$$u_R = \frac{\hat{u} - \hat{u}_2}{\hat{u}_1 - \hat{u}_2} \tag{53}$$

We use the definition $s = u_R(y_s)$ for y_s and denote δ by $\delta = y_{0.9} - y_{0.1}$. Using δ, we normalize y as

$$y_R = (y - y_{0.5})/\delta \tag{54}$$

The growth rate of the layer G is defined by $\mathrm{d}\delta/\mathrm{d}x$.

In the following computation of a plane free-shear layer flow, we consider the case

$$\gamma_u = \tfrac{1}{2}, \qquad \gamma_\rho = 1, \qquad \gamma_e = 1 \tag{55}$$

The last two indicate that $\bar{a}_1 = \bar{a}_2 = a$, which is used as the reference velocity for normalizing the velocity.

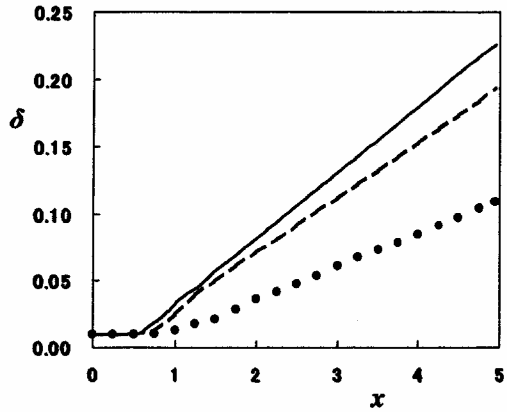

Fig. 1 Growth of a free-shear layer: ——, standard K-ε model at $M_C = 0$; - - -, present model with C_N = 0.8 and C_M = 0 at M_C = 0; and ●●●, present model with C_N = 0.8 and C_M = 30 at M_C = 1.

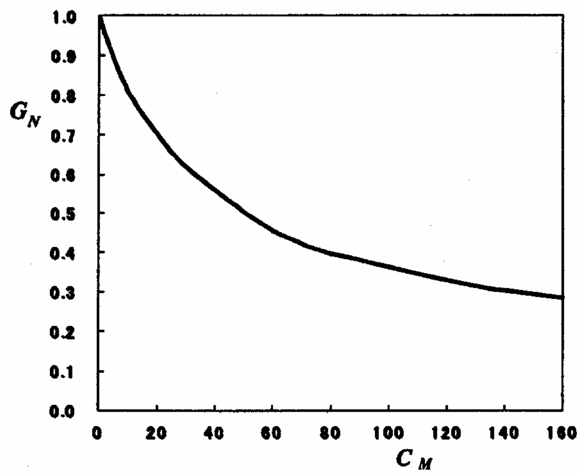

Fig. 2 Dependence of the normalized growth rate G_N on C_M with C_N = 0.8.

We first examine the relationship of the present nonequilibrium effect with a free-shear layer flow in the low-Mach-number limit. In Eq. (40a), we set $C_M = 0$ and consider the case of $\gamma_u = \frac{1}{2}$, as in Eq. (55). The dependence of δ on the downstream location x is given in Fig. 1. Here, the growth rate in the low-Mach-number limit G_L is $G_L = 0.041$, whereas the standard $K - \varepsilon$ model with $C_N = C_M = 0$ gives $G_L = 0.048$.

The observed growth rate $G_{\rm LO}$ scatters considerably according to different conditions, such as the upstream condition. The conditions are arranged into an empirical formula[36]:

$$S = \frac{\hat{u}_1 + \hat{u}_2}{2(\hat{u}_1 - \hat{u}_2)} G_{\rm LO} \tag{56}$$

with

$$0.06 < S < 0.11 \tag{57}$$

In the present situation, with $\gamma_u = \frac{1}{2}$, Eqs. (56) and (57) give

$$0.04 < G_{\rm LO} < 0.073 \tag{58}$$

The foregoing two G_L fall in this range, although they are close to the lower limit. The renormalized mean velocity u_R [Eq. (53)] will be shown later for the case of nonvanishing M_C.

Next, we consider the supersonic-effect parameter C_M in Eq. (40). Under condition (55), we examine the case

$$\hat{u}_1 = 4, \qquad \hat{u}_2 = 2, \qquad M_C = 1 \tag{59}$$

where the velocity was nondimensionalized using the sound velocity in the freestreams. We normalize the growth rate by the low-Mach-number counterpart as $G_N = G/G_L$. Figure 2 shows the dependence

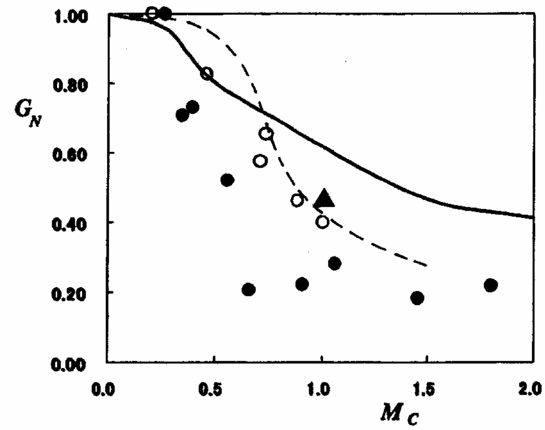

Fig. 3 Dependence of the normalized growth rate on the convective Mach number: ——, present model with C_N = 0.8 and C_M = 30 (▲, C_M = 60); - - -, Langley curve (see Ref. 2); ●●●, Papamoschou and Roshko[38]; and ○○○, Goebel and Dutton.[39]

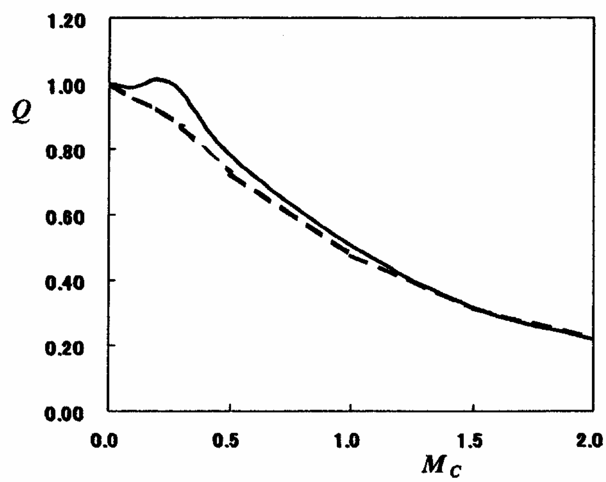

Fig. 4 Integrated turbulent energy and dissipation rate vs the convective Mach number: ——, $Q\{\bar{\rho}K\}$ and - - -, $Q\{\bar{\rho}\varepsilon\}$.

of G_N on C_M. Note that the decrease in G_N is large for small C_M and becomes gradual for $C_M \geq 30$. We adopt $C_M = 30$. For this choice of C_M, the growth line of the shear layer at $M_C = 1$ is added in Fig. 1.

For $C_M = 30$, we examine the normalized growth rate G_N for various convective Mach numbers. The computed results are given in Fig. 3, with some observations.[37,38] The former behavior is consistent with the latter, although the computed suppression rate is rather smaller than the observational results. For larger C_M, for instance, $C_M = 60$ gives $G_N \cong 0.4$ at $M_C = 1$. (See the triangle in Fig. 3.) The G_N curve becomes much closer to the Langley curve and observations. In this stage, we cannot single out the most appropriate value of C_M. Its optimization is left for further study of different flows. The present computed results, however, clearly indicate that the newly introduced parameter χ [Eq. (33)] is instrumental in capturing this important feature of the growth rate in a supersonic free-shear layer flow, without generating undesirable effects on a channel flow.

To see the reduction in K and ε due to supersonic effects, we introduce

$$Q\{f\} = \frac{\int_{-\delta}^{\delta} f \, \mathrm{d}y}{\left(\int_{-\delta}^{\delta} f \, \mathrm{d}y\right)_{M_C = 0}} \tag{60}$$

As f, we adopt $\bar{\rho}K$ or $\bar{\rho}\varepsilon$ at $x = 5$ in Fig. 1. For $\bar{\rho}K$ and $\bar{\rho}\varepsilon$, Q are plotted in Fig. 4. The tendency of reduction with increasing M_C is consistent with the DNSs of homogeneous-shear and free-shear layer flows, but the present reduction rate is larger. This is due to the limitation of this modeling in which χ effects are taken into account through ν_T only. The normalized mean velocity u_R is insensitive to

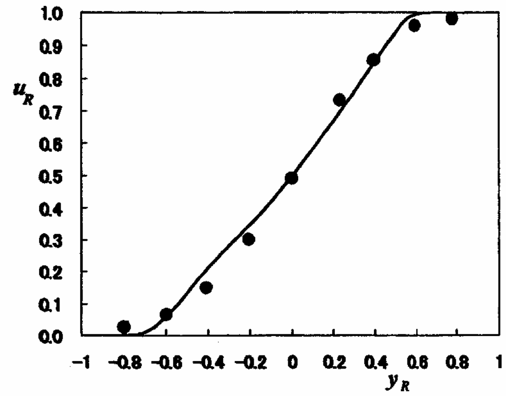

Fig. 5 Normalized mean velocity: ——, present model with C_N = 0.8 and C_M = 30 and ●●●, Samimy and Elliot.[40]

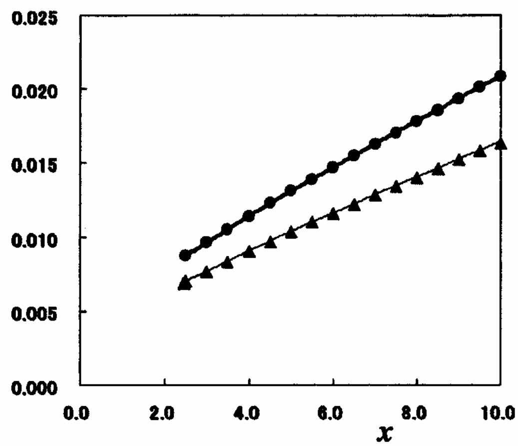

Fig. 6 Growth rates of the displacement (δ_D) and momentum (δ_M) thickness in a turbulent boundary layer at M_∞ = 2: ——, δ_D for C_N = 0 and C_M = 0; ——, δ_M for C_N = 0 and C_M = 0; ●●●, δ_D for C_N = 0.8 and C_M = 30; and ▲▲▲, δ_M for C_N = 0.8 and C_M = 30.

the magnitude of M_C. As a typical example, we give u_R under the conditions set in Eq. (55) in Fig. 5, which is compared with the observational result[39] for $M_C = 0.5$.

B. Supersonic Boundary-Layer Flow

In the foregoing discussions, we paid special attention to two typical flows concerning the streamwise variation of flow properties, that is, channel and free-shear layer flows. The proposed turbulent supersonic effect vanishes identically in the former, whereas it plays a critical role in the suppression of the growth rate in the latter. Note that an intermediate flow is a supersonic boundary-layer flow. There, the D/Dt-related effects survive, although they are expected to be small compared with those in a free-shear layer flow. It is known that the primary mean-flow properties of a supersonic boundary-layer flow are similar to those of a channel flow and may be reproduced through the proper treatment of the variation of mean density. Then it is important to confirm that the present nonequilibrium model does not give rise to any spurious effects in the analysis of a supersonic boundary-layer flow.

To confirm that a boundary-layer flow is insensitive to the present supersonic effect, we use the $K-\varepsilon$-type model of Myong et al.[40] and replace only the equilibrium part of the turbulent viscosity with the present nonequilibrium turbulent viscosity, Eq. (40a). The Sutherland formula is adopted for the temperature variation of the viscosity μ.

We apply the forgoing modified model to a supersonic boundary-layer flow at $M_\infty = 2$. (M_∞ is the freestream Mach number.) The computed displacement and momentum thickness are shown in Fig. 6, along with that computed by the original model of Myong et al.[40] These results indicate that the present nonequilibrium effect hardly affects the boundary-layer growth. This computational result signifies that the mean-flow properties of a supersonic boundary-layer flow may be computed without any spurious supersonic effects. Then the present model fulfills requirement 1 in Sec. I. The accuracy of computed results depends on that of a turbulent-viscosity model for low-Mach-number flow.

VI. Conclusions

In this work, we proposed a supersonic turbulence model based on the nonequilibrium turbulent viscosity and tested it for two typical turbulent flows, that is, free-shear layer and boundary-layer flows. As a result, we succeeded in reproducing some representative features of a free-shear layer flow, such as the suppression of growth rate with an increasing convective Mach number, without generating undesirable supersonic effects on a boundary-layer flow. This is the first step toward resolving the difficulty in analyzing free-shear layer and wall-bounded flows by one model. In the present stage of testing, however, the selection of the model constants linked with nonequilibrium and supersonic effects has not been fully explored yet. In general, turbulent-viscosity models are insufficient for expressing anisotropic turbulence properties. For rectifying such a shortfall, we need to extend the present model to a model of the explicit algebraic nonlinear type. Such an extension and the application to various supersonic flows are left for future work.

Acknowledgments

The authors are grateful to the referees for improving the presentation of the manuscript.

References

[1] Settles, G. S., and Dodson, L. J., "Hypersonic Turbulent Boundary Layer and Free Shear Databases," NASA CR 177610, 1993.

[2] Kline, S. J., Cantwell, B. J., and Lilley, G. M., *1980-1981 AFOSR–HTTM–Stanford Conference on Complex Turbulent Flows*, Stanford Univ. Press, Stanford, CA 1981.

[3] Zeman, O., "Dilatation Dissipation: The Concept and Application in Modeling Compressible Mixing Layer," *Physics of Fluids A*, Vol. 2, No. 2, 1990, pp. 178–188.

[4] Sarkar, S., Erlebacher, G. E., Hussaini, M. Y., and Kreiss, H. O., "The Analysis and Modeling of Dilatational Terms in Compressible Turbulence," *Journal of Fluid Mechanics*, Vol. 27, 1991, pp. 473–493.

[5] Sarkar, S., "The Pressure–Dilatation Correlation in Compressible Flows," *Physics of Fluids A*, Vol. 4, No. 12, 1992, pp. 2674–2682.

[6] Liou, W. W., Shih, T.-H., and Duncan, B. S., "A Multiple-Scale Model for Compressible Turbulence," *Physics of Fluids*, Vol. 7, No. 3, 1995, pp. 658–666.

[7] Shyy, W., and Krishnamurty, V. S., "Compressibility Effects in Modeling Complex Turbulent Flows," *Progress in Aerospace Science*, Vol. 33, No. 9–10, 1997, pp. 587–645.

[8] Ristorcelli, J. R., "A Pseudo-Sound Constitutive Relationship for the Dilatational Covariances in Compressible Turbulence," *Journal of Fluid Mechanics*, Vol. 347, 1997, pp. 37–70.

[9] Taulbee, D., and VanOsdol, J., "Modeling Turbulent Compressible Flows: The Mass Fluctuating and Squared Density," AIAA Paper 91-0524, Jan. 1991.

[10] Sarkar, S., "The Stabilizing Effect of Compressibility in Turbulence," *Journal of Fluid Mechanics*, Vol. 282, 1995, pp. 161–186.

[11] Vreman, A. W., Sandham, N. D., and Luo, K. H., "Compressible Turbulent Mixing Layer Growth Rate and Turbulence Statistics," *Journal of Fluid Mechanics*, Vol. 320, No. 1996, pp. 235–258.

[12] Freund, J. B., Lele, S. J., and Moin, P., "Compressibility Effects in a Turbulent Annular Mixing Layer. Part 1. Turbulence and Growth Rate," *Journal of Fluid Mechanics*, Vol. 421, 1996, pp. 229–267.

[13] Adumitroaie, V., Ristorcelli, J. R., and Taulbee, D. B., "Progress in Favré–Reynolds Stress Closures for Compressible Flows," *Physics of Fluids*, Vol. 10, No. 9, 1999, pp. 2696–2719.

[14] Fujiwara, H., Matsuo, Y., and Arakawa, C., "A Turbulence Model for the Pressure–Dilatation Correlation Term Accounting for Compressibility Effect," *International Journal of Heat and Fluid Flow*, Vol. 21, No. 3, 2000, pp. 354–358.

[15] Coleman, G. N., Kim, J., and Moser, R. D., "A Numerical Study of Turbulent Supersonic Isothermal-Wall Channel Flow," *Journal of Fluid Mechanics*, Vol. 305, 1995, pp. 159–183.

[16] Bradshaw, P., "Turbulence Modeling with Application to Turbomachinery," *Progress in Aerospace Science*, Vol. 32, No. 6, 1996, pp. 575–624.

[17]Rubinstein, R., and Erlebacher, G., “Transport Coefficients in Weakly Compressible Turbulence,” *Physics of Fluids*, Vol. 9, No. 10, 1997, pp. 3037–3057.

[18]Hamba, F., ”Effects of Pressure Fluctuations on Turbulence Growth in Compressible Homogeneous Shear Flow,” *Physics of Fluids*, Vol. 11, No. 6, 1999, pp. 1623–1635.

[19]Yoshizawa, A., and Nisizima, S., “A Nonequilibrium Representation of the Turbulent Viscosity Based on a Two-Scale Turbulence Theory,” *Physics of Fluids A*, Vol. 5, No. 12, 1993, pp. 3302–3304.

[20]Yoshizawa, A., “Nonequilibrium Effect of the Turbulent-Energy-Production Rate Process on the Inertial-Range Spectrum,” *Physical Review E*, Vol. 49, No. 5-A, 1994, pp. 4065–4071.

[21]Yoshizawa, A., “Statistical Analysis of the Deviation of the Reynolds Stress from Its Eddy-Viscosity Approximation,” *Physics of Fluids*, Vol. 27, No. 6, 1984, pp. 1377–1387.

[22]Hamba, F., “Statistical Analysis of Chemically Reacting Passive Scalars in Turbulent Shear Flows,” *Journal of the Physical Society of Japan,* Vol. 56, No. 1, 1987, pp. 79–96.

[23]Yoshizawa, A., *Hydrodynamic and Magnetohydrodynamic Turbulent Flows: Modelling and Statistical Theory*, Kluwer, Dordrecht, The Netherlands, 1998, pp. 173–253.

[24]Okamoto, M., “Theoretical Investigation of an Eddy-Viscosity-Type Representation of the Reynolds Stresses,” *Journal of the Physical Society of Japan*, Vol. 63, No. 6, 1994, pp. 2102–2122.

[25]Taulbee, D. B., “An Improved Algebraic Stress Model and Corresponding Nonlinear Stress Model,” *Physics of Fluids A*, Vol. 4, No. 11, 1992, pp. 2555–2561.

[26]Gatski, T. B., and Speziale, C. G., “On Explicit Algebraic Stress Models for Complex Turbulent Flows,” *Journal of Fluid Mechanics*, Vol. 254, 1993, pp. 59–78.

[27]Girimaji, S. S., “Fully Explicit and Self-Consistent Algebraic Reynolds Stress Model,” *Theoretical and Computational Fluid Dynamics*, Vol. 8, No. 6, 1996, pp. 387–402.

[28]Craft, T. J., Launder, B. E., and Suga, K., “Development and Application of a Cubic Eddy-Viscosity Model of Turbulence,” *International Journal of Heat and Fluid Flow*, Vol. 17, No. 2, 1996, pp. 108–115.

[29]Abe, K., Kondoh, T., and Nagano, Y., “On Reynolds-Stress Expressions and Near-Wall Scaling Parameters for Predicting Wall and Homogeneous Turbulent Shear Flows,” *International Journal of Heat and Fluid Flow*, Vol. 18, No. 3, 1997, pp. 266–282.

[30]Speziale, C. G., and Mac Giolla Mhuiris, N., ”On the Prediction of Equilibrium States in Homogeneous Turbulence,” *Journal of Fluid Mechanics*, Vol. 209, 1989, pp. 591–615.

[31]Yoshizawa, A., Liou, W. W., Yokoi, N., and Shih, T.-H., “Modeling of Compressibility Effects on the Reynolds Stress Using a Markovianized Two-Scale Method,” *Physics of Fluids*, Vol. 9, No. 10, 1997, pp. 3024–3036.

[32]Yoshizawa, A., “Statistical Theory of Compressible Turbulence Based on Mass-Weighted Averaging, with an Emphasis on a Cause of Countergradient Diffusion,” *Physics of Fluids*, Vol. 15, No. 3, 2003, pp. 585–596.

[33]Yao, Y. F., Thomas, T. G., Sandham, N. D., and Williams, J. J. R., “Direct Numerical Simulation of Turbulent Flow over a Rectangular Trailing Edge,” *Theoretical and Computational Fluid Dynamics*, Vol. 14, No. 5, 2001, pp. 337–358.

[34]Yoshizawa, A., “Statistical Analysis of Mean-Flow Effects on the Pressure–Velocity Correlation,” *Physics of Fluids*, Vol. 14, No. 5, 2002, pp. 1736–1744.

[35]Suga, K., “Modelling of Turbulent Pressure-Diffusion Effects,” *Proceedings of the 16th Symposium on Computational Fluid Dynamics*, Japan Society of Fluid Mechanics, Tokyo, 2002, p. 213.

[36]Dimotakis, P. E., “Turbulent Free Shear Mixing and Combustion,” *High-Speed Flight Propulsion Systems*, edited by S. N. B. Murthy and E. T. Curran, Vol. 137, Progress in Astronautics and Aeronautics, AIAA, Washington, DC, 1991, pp. 265–340.

[37]Papamoschou, D., and Roshko, A., “The Compressible Turbulent Shear: An Experimental Study,” *Journal of Fluid Mechanics*, Vol. 197, 1988, pp. 453–477.

[38]Goebel, S. G., and Dutton, J. C., “Experimental Study of Compressible Mixing Layers,” *AIAA Journal*, Vol. 29, No. 4, 1991, pp. 538–546.

[39]Samimy, M., and Elliott, G. S., “Effects of Compressibility on the Characteristics of Free Shear Layers,” *AIAA Journal*, Vol. 28, No. 3, 1990, pp. 439–445.

[40]Myong, H. K., Kasagi, N., and Hirata, M., “A New Approach to the Improvement of k–ε Turbulence Model for Wall-Bounded Shear Flows,” *JSME International Journal*, Vol. 33, No. 1, 1990, pp. 63–72.

R. M. C. So
Associate Editor